WIND TUNNEL EXPERIMENTATION OF ICE PARTICLES TRANSPORT IN MARTIAN-LIKE ENVIRONMENT

C. Herny[1] , J. Merrison[2], J. Iversen[2], Z. Yoldi[3], M. Bordiec[4], S. Carpy[4], O. Bourgeois[4], and N. Thomas[1], [1]Physikalisches Institut, Universität Bern, Sidlerstrasse 5, 3012 Bern, Switzerland (clemence.herny@space.unibe.ch), [2]Departement of Physics and astronomy, Aarhus University, Ny Munkegade 120, 8000 Aarhus C, Denmark, [3]Niels Borh Institute, Tagensvej 16, 2200 København N, Denmark, [4]Laboratoire de Planétologie et Géodynamique - UMR CNRS 6112, Université de Nantes, 2 rue de la Houssinière - BP 92208, 44322 Nantes Cedex 3, France

Introduction: The transport of ice by wind plays a major role in the surface mass balance of polar caps [1, 2]. Ice can be redistributed by wind due to (1) transport of ice particles and/or (2) transport of water vapour associated with sublimation/condensation. On Mars, although the low atmospheric density is less favorable for the transport of particles than on Earth, both dust and sand have been observed to be transported by wind [3,4]. Despite ice Aeolian landforms have been observed at the surface of the North Polar Cap of Mars [2, 5, 6], ice particle transport has not been directly observed on the Martian surface. Similarly, no laboratory studies of snow/ice particle transport under Martian-like conditions (even at pressure lower than 1000 mbar) have been attempted thus far due to the complexity of the material. In this study we performed experiments of ice particle transport in a wind-flow under low temperatures and low pressures. From the experiments, threshold shear velocity of water ice particle transport is retrieved for different pressures and particle shapes and sizes in order to evaluate the plausibility of ice particle wind-driven transportation at the surface of Mars.

The North Polar Cap of Mars: The Martian atmosphere is thin (7 mbar), cold (220 K) and dry (< 80 µm-pr) [7]. These conditions favored ice sublimation/condensation processes. The polar caps are made of a mixture of ice and dust. Spectral analyses [8, 9] suggested the optical grain sizes to vary between 10 µm to about 2000 µm for the seasonal frost and surface of the perennial North polar cap. But, the mechanisms of ice deposition are not well established. It can potentially come from vapour condensation directly onto the surface [9] or from snow fall [10]. This will affect the shape and size of ice particles and degree of ice sintering, which all influence the shear velocity threshold. The North polar cap experiences a permanent katabatic wind regime [11] with a typical friction shear velocity u_* about 0.2 m.s^{-1}. The complex interactions between the cryosphere and the wind leads to the formation of Aeolian features at different scales [2, 5, 6].

Wind tunnel experiments: We performed experiments using the environmental wind tunnel AWTSII at Aarhus University. It is a cylindrical vacuum chamber, housing a recirculating wind tunnel about 8 m long, 2 m wide and 1 m high [12]. The facility can achieve a turbulent boundary layer flow at both low temperature and low pressure. The ice samples were produced by crushing ice blocks (irregular and angular shape particles) and by using the Setup for production of Icy Planetary Analogues (SPIPA, spherical shape particles) [13]. The ice samples were sieved (125 - 250 µm, 250 - 500 µm, 500 - 2000 µm) as a monolayer on a sample plate (20 cm x 20 cm) cover with volcanic regolith (125 µm). The fan speed was increased by steps (shear velocity u_* = 0 to 2 m.s^{-1}) and the wind flow characterized by laser Doppler anemometry. The removal of ice particles was monitored by webcam**.** We performed the experiments for the different particle shapes and sizes for 4 different air pressures; 40, 100, 500 and 1000 mbar. The air temperature was maintained low (~-25°C) close to the sample plate to prevent the ice melting, sublimating and sintering.

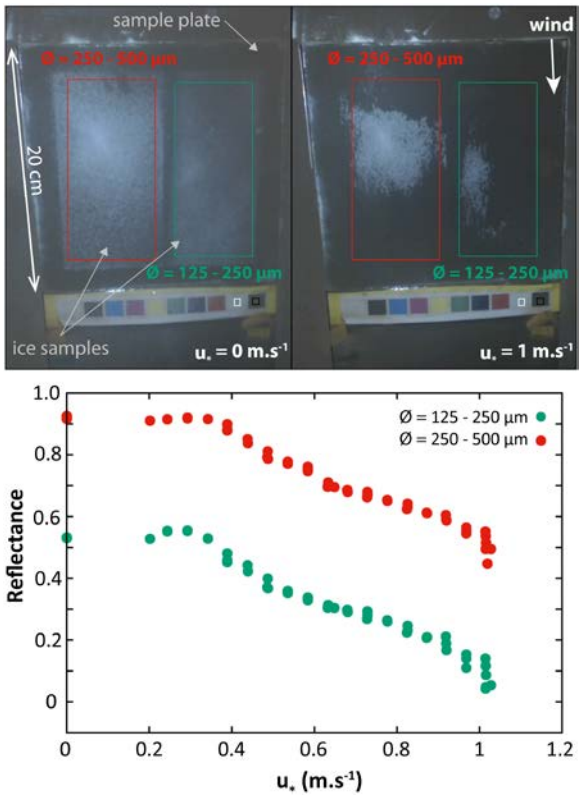

Figure 1: Images of the ice samples (SPIPA) evolution from $u_* = 0$ m.s^{-1} (up left, beginning of the experiment) to $u_* = 1$ m.s^{-1} (up right, end of the experiment). Two ice samples, with different particles sizes (125 – 250 µm and 250 – 500 µm respectively on the right and on the left) are observed side by side. For both grain sizes, ice particles have been removed by wind. The wind comes from the top to the bottom of the images. The experiment is performed at P = 500 mbar and T ~-25°C. A color bar is placed near the sample plate to calibrate the reflectance of the regions of interest defined on the ice samples (green and red boxes). The reflectance decreases as the shear velocity increases for both ice particles sizes (lower plot). The estimated threshold shear velocity in both case is about 0.4 m.s^{-1}.

Threshold shear velocity calculation: The threshold shear velocity was determined from analysis of acquired images. When bright ice particles are removed from the dark volcanic regolith sample plate, the reflectance of the surface decreases (Fig. 1). Black and white reference targets are placed close to the sample plate in the field of view of the webcam. The reflectance evolution of a region of interest (ROI) on the sample plate is calculated as follow:

$$\text{reflectance} = (\text{ROI} - \text{black target}) / (\text{white target} - \text{black target})$$

The reflectance serve as a proxy for ice mass removal. For each image the reflectance is linked to the corresponding shear velocity. In the case of Fig. 1, the reflectance is constant until a certain wind speed and then decreases. To determine the threshold shear velocity u_{th}, we set the threshold reflectance at 10% decrease from the first image at $u_* = 0$ m.s^{-1}.

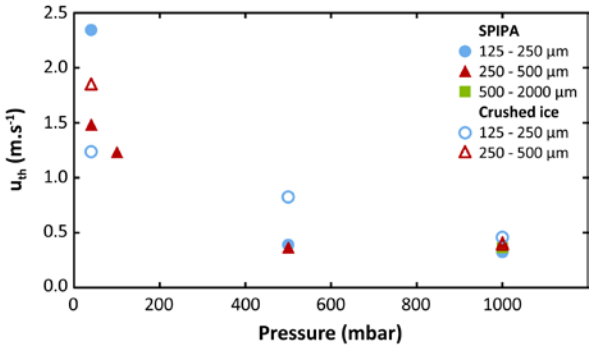

Figure 2: Threshold shear velocity evolution with wind tunnel air pressure for different ice particles production and sizes.

Results: Figure 2 shows preliminary results of the threshold shear velocity evolution with air pressure for different grain sizes and shapes. The averaged value obtained at 1000 mbar, $u_{th} = 0.4$ m.s^{-1}, is consistent with theoretical and experimental calculation of ice/snow at terrestrial condition [14, 15], from 0.3 m.s^{-1} to 0.6 m.s^{-1} for range of ice particles sizes selected, supporting our set-up reliability. The shear velocity increases significantly as the pressure decreases. The ice grain shapes and sizes appear to have a influence at lower pressure while no significant effect is highlighted at terrestrial pressure. However more replicates should be perform at low pressures to better characterized u_{th}.

Conclusion and future work: We have performed for the 1st time experiments of ice particles transportation at low pressure in a planetary wind tunnel. These preliminary results show an increase of threshold shear velocity as the pressure decreases. The conclusions should be reinforced with additional measurements and then be scaled to Martian gravity in order to conclude about the likeliness of transport of ice particles by wind at the surface of Mars. In case results reveal that the transport of ice particles under Martian condition is unlikely, we plan to experimentally explore the second hypothesis of ice mass redistribution which is the transport of water vapour associated with sublimation/condensation that is also thought to have a strong influence on the polar caps of Mars [16, 17].

References: [1] Das I. et al. (2013) *Nature Geoscience*, *6*, 367-371. [2] Howard A. D. (2000) *Icarus*, *144*, 267-288. [3] Cantor B. A. et al. (2010) *Icarus*, *208*, 61-81. [4] Bridges B. A. et al. (2012) *Geology*, *40*, 31-34. [5] Smith I. B. and Holt J. (2010) *Nature*, *465*, 450-453. [6] Herny C. et al. (2014) *EPSL*, *403*, 56-66. [7] Pankine A. A. et al. (2010) *Icarus*, *210*, 5871. [8] Langevin Y. et al. (2005) *Science*, *307*, 1584-6. [9] Appéré T. et al. (2011) *JGR : Planets*, *116*, E05001. [10] Spiga A. et al. (2017) *Nature Geoscience*, *10*, 652-657. [11] Spiga A. et al. (2011) *PSS*, *59*, 915-922. [12] Holstein-Rathlou C. et al. (2014) *Am. Met. Society*, *31*, 447-457. [13] Pommerol A. et al. (2019) *Space Sci. Rev.*, *215*. [14] Shao Y. and Lu H. (2000) JGR, *105*, 437-443. [15] Clifton A. et al. (2006) *JoG*, *52*, 585-596. [16] Herny C. et al. (2016) 6th MPSC, Abstract #6075. [17] Bordiec M. et al. (2018) ICAR X.

Acknowledgements: This work has been fund by Europlanet (Europlanet 2020 RI has received funding from the European Union's Horizon 2020 research and innovation program under grant agreement No 654208). This work has been supported by the University of Bern. This work has been carried out within the framework of the NCCR PlanetS supported by the Swiss National Science Foundation.